

Autonomous healing by vascular networks: tracking of cracks interaction by Ultrasounds and Acoustic Emission

Eva Vangansbeke¹, Yasmina Shields², Nele De Belie², Kim Van Tittelboom² and Eleni Tsangouri^{1}*

¹ Department of Mechanics of Materials and Constructions (MeMC), Vrije Universiteit Brussel (VUB), Pleinlaan 2, 1050 Brussels, Belgium; Eleni.Tsangouri@vub.be

² Magnel-Vandepitte Laboratory, Department of Structural Engineering and Building Materials, Faculty of Engineering and Architecture, Ghent University, Technologiepark Zwijnaarde 60, 9052 Ghent, Belgium

Abstract. The tracking of healing on concrete slabs where dense crack patterns are formed under bending is reported using Acoustic Emission (AE) and Ultrasound Pulse Velocity (UPV). Additively manufactured polymeric networks are designed to distribute a polyurethane agent through capillary actions and under pressure to the open cracks, formed in the slabs. It is shown that the crack pattern is controlled by the geometry of the vascular networks that are positioned near the steel reinforcement. The activation of both conventional linear and interlinked web-shaped networks is monitored by AE, however in both cases the load at which the initial cracks form is lower in series with embedded networks compared to the reference series, an indication of an overall weakening effect. The area where the healing agent circulates is larger (300x400 mm²) than past tests on beams, but only local healing is evident by UPV mapping. An indirect proof of cracks filling with stiffened agent is provided by the AE pencil-lead breaking test, as the amplitude recovery after healing can be linked to crack closure. This preliminary work evaluates the design of 3D printed vascular networks, but also explores the potential of AE and UPV as inspection tools in healing studies.

1 Introduction

A second generation of research on the design of autonomously healing concrete emerges in the current state-of-the-art [1], with particular progress being made in the implementation of 3D printed pre-fixed vascular networks in concrete [2]. Among others, the work of Di Nardi et al. [3] and our recent work [4] report on the enhanced performance of concrete in which additively manufactured polymeric brittle tubes are embedded that form a distributor for the healing agent that partially seals the cracks, a system that appears promising for repeatable healing.

Recent reviews of current design solutions [5,6] report on a plethora of network-casting materials developed with paramount geometrical complexity, numerous agent solutions with varying response to stress, but most importantly highlighting the lack of standardized test procedures for qualitative and quantitative healing assessment [7]. As a result, the majority of studies evaluate the proposed healing concepts using small-scale mortar prisms or larger scale beams (i.e. [8]), however these linear elements break in a controlled manner or in a restricted zone. In real-life conditions, the performance of self-healing concrete will be evaluated in large-scale bulk concrete structural elements where multiple cracks dynamically develop and interact after healing leading to very complex fracture phenomena [9]. For this reason, the testing configuration needs to be adapted to the complexity of

the crack patterns and the three-dimensional response of vascular networks to cracking.

1.1 Research objectives

The research introduced in this paper aims to develop a standardized test protocol that will comprehensively report on the performance of novel self-healing vascular networks. For this reason, two elastic-wave based non-destructive monitoring methods are applied, the Acoustic Emission (AE) and the Ultrasound Pulse Velocity (UPV, previously established in [10-11]). These techniques have been used previously during repeatable cracking cycles and after healing interventions to assess the fracture progress and the healing efficacy. A conventional, linear vascular network (like in [12-13]) is compared to a more experimental design, both embedded in small-scale slabs and loaded in four-point bending. This way, for the first time in literature, the self-healing design is explored not in linear, but in planar perspective considering the cracking kinetics and interaction with the networks.

2 Materials and Methods

The test campaign is the core work of the Master thesis of E. Vangansbeke (VUB) and the extended results and analysis can be consulted there [15]. In total, 15 concrete slabs were cast to explore the performance of different network designs (i.e. brittle and flexible-not explored in this work- 3D printed polymers). Among them, three

series, summarized in Table 1, are selected to be further discussed in this paper.

Table 1. Slab series under investigation.

Series name	Samples	Description
Reference (REF)	3	No vascular network
Conventional (CONV)	3	2 pairs of linear tubes mounted on rebars
Experimental (EXP)	3	Inter-connected tubes mounted on rebars

The concrete samples are designed as small-scale slabs carrying a minimum of steel reinforcement to ensure that numerous cracks are formed and distributed in the area covered by the vascular networks. For the first time in literature, the vascular networks are extended to plate geometries (until now mainly beam geometries have been considered). Slab's design ensures that multiple cracks are triggered, extended and interconnected along the concrete's depth, and eventually evaluated for healing.

2.1 Concrete design and casting

The concrete slabs have dimensions of 450 x 300 x 55 mm and are reinforced by 4 Φ 8 ribbed steel rebars. The mixing composition is reported in Table 2 and is designed based on the mix design used for an interlaboratory test campaign performed by SARCOS [7]. The dry ingredients are mixed for 1 minute and then the water and superplasticiser are progressively added reaching a total mixing duration of 3 minutes.

Table 2. Concrete composition.

Component	Quantity	Component	Quantity
Cement CEM I 52.5 N	337.6 kg/m ³	Gravel 2/8	1013.1 kg/m ³
Water	185.2 l/m ³	Limestone filler	58 kg/m ³
Sand 0/2	742.5 kg/m ³	Superplasticizer	1328 ml/m ³

The concrete is poured into the wooden moulds where the rebars are pre-fixed at 20 mm above the bottom with an intermediate distance of 60 mm. The vascular networks are also pre-fixed, mounted below the rebars, as discussed in Section 2.2. The slabs are demoulded 24 hours after casting and cured under water in approximately 20°C for 27 days more before testing.

2.2 Vascular networks

The network tubes are 3D printed perpendicular to the build slab using polylactic acid (PLA) filaments via fused deposition modelling (FDM). All designed tubes

are ribbed and have a diameter of 7 mm, and a wall thickness of 1.6 mm (optimal design according to preliminary tests of tube fracture under bending for small-scale mortar beams).

Conventional series: Two pairs of networks are built with each network consisting of two ribbed tubes developing in parallel along the slab's length debouching in an outlet at each side. The networks are cast in three pieces as depicted in Figure 1a and glued together with Tec7 MSPolymer glue to ensure connection sealing. The networks are pre-fixed at the bottom of the steel rebars using fine wires.

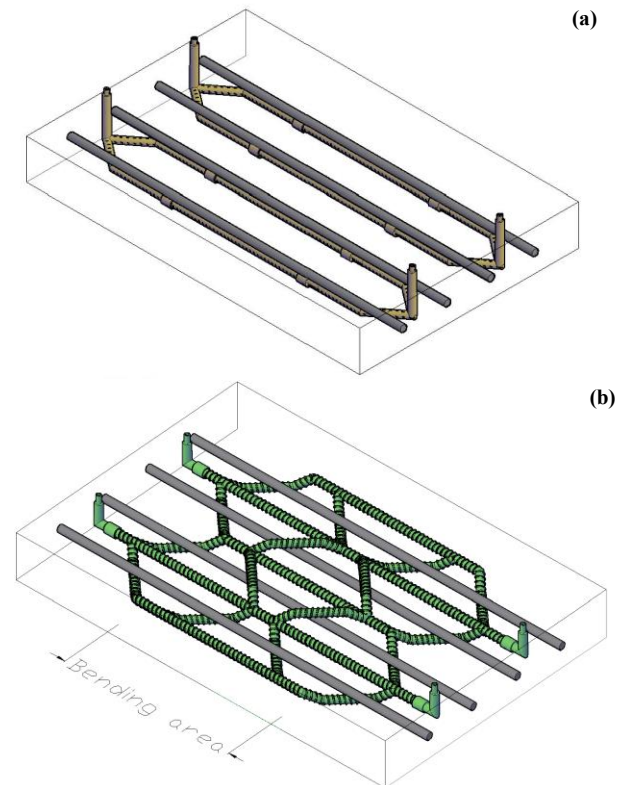


Fig. 1. a) 3D model of the conventional network mounted below the steel rebars; b) 3D model of the experimental vascular network design.

Experimental series: A more complex network alignment is depicted in Figure 1b, where the printed networks are this time inter-linked as one tube is split in three branches at the edges of the bending zone and further reaches one central tube at the middle of the slab. The network envelops the reinforcement bars providing a network distribution at the cover and above the rebars. This way, the crack sealing can be achieved along different heights of the slab.

The polyurethane healing agent used in this study is selected based on a parametric performance study with rheological, physical and mechanical properties reported in [15].

2.3 Four-point bending

The slabs are loaded under four-point bending using an Instron 5900R testing bench and load cell with a capacity of 100 kN. The supporting span is equal to 410 mm, whereas the bending span is fixed at 200 mm.

The applied load is transferred from the pins with a length of 200 mm along the width of the slabs using metal plates (50 mm wide; 300 mm long) placed in between the slab and the pins. The loading pins are moving downwards with a displacement rate of 0.5 mm/min and unloading is performed manually with an approximate rate of 1 mm per minute.

The first bending cycle ends as soon as the plateau of plastic deformation is reached and if at least one of the cracks is wider than 500 μm at the bottom of the slab. The crack opening is tracked by Digital Image Correlation that monitors the side view of the plates. As a result, at least one crack is wider than 300 μm after unloading and up to 6 cracks were reported with openings varying from 50 to 500 μm.

After testing, the healing agent is poured into the networks and, with the aid of manually-controlled pressure, it flows and eventually reaches the cracks. After 30 min, the agent is flushed out of the networks under pressure using water. A second bending cycle follows 24 hours later using the same testing configuration and control method. Healing agent is re-flushed for a second time afterwards and a final third cycle of cracking (re-cracking after re-healing cycle) follows at least a month after the second testing cycle to explore potential re-healing.

2.4 Acoustic Emission

An array of six AE transducers are mounted on the side (5 and 6, Figure 2) and the bottom (1 to 4, Figure 2) of each slab, covering the entire bending zone. The transducers are provided by Mistras and have a resonant frequency response at 150 kHz. Their diameter is 13 mm, their contact with concrete is enhanced by a layer of coupling agent (Vaseline grease) and the transducers are fixed in place during testing using magnetic holders. A pre-amplification of 40 dB is adopted and the amplitude threshold is set at 39 dB, whereas the sampling frequencies are limited between 20 kHz and 1 MHz. The AE hits are registered using the AEwin software. Among AE wave features, the signal strength is selected to be discussed in this work as an indicator of the damage magnitude. The hits analysis is synchronized to the Instron load.

Before and after each testing cycle, and in order to ensure the AE transducers are at a fixed position, a pencil lead breakage test is done according to the Hsu-Nielsen protocol [16]. The data collected in this calibration analysis is also presented in this work since the amplitude of the AE hits triggered by pencil lead breakage close to sensor 1 and collected from opposing sensor 4 can demonstrate the damage condition between these sensors as depicted in Figure 2. It is expected that the amplitude is recovered after healing and drops again at the end of each loading cycle.

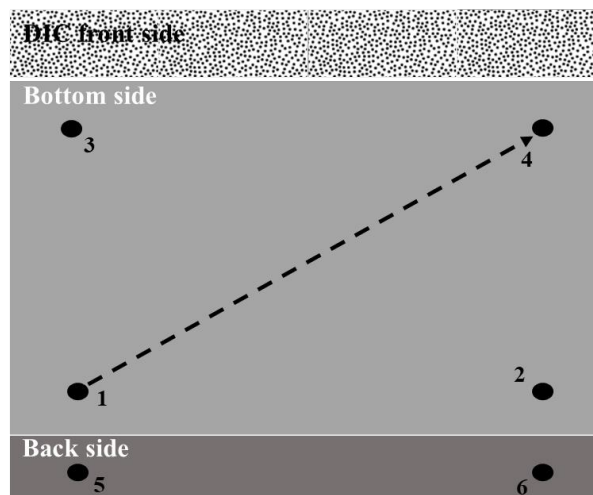


Fig. 2. Acoustic Emission transducers setup with the sensors' 1-4 path considered during pencil lead breaking.

2.5 Ultrasound Pulse Velocity

The ultrasound pulse velocity (UPV) is measured through the thickness of the slab at a series of points with a grid outline as depicted in Figure 3. The transit time (in μs) is measured between emitter and receiver probes placed facing each other at the bottom and top side of the slab respectively. A pulse generator device sends a signal of 2500 V with a frequency of 54 kHz, which is recorded by the receiver with a sampling rate of 10 MHz. With a known propagation distance (equal to 55 mm), the velocity is measured and projected in a color mapping that reports on concrete quality and cracking: healthy/healed: UPV > 3900 m/s; cracked: 3900 > UPV > 2500 m/s; severely damaged and unhealed: UPV < 2500 m/s.

It is noted that only the UPV measured after the second healing cycle is presented in this work since at that moment the greatest healing performance is expected; the recovered zones are depicted and compared to unhealed reference series.

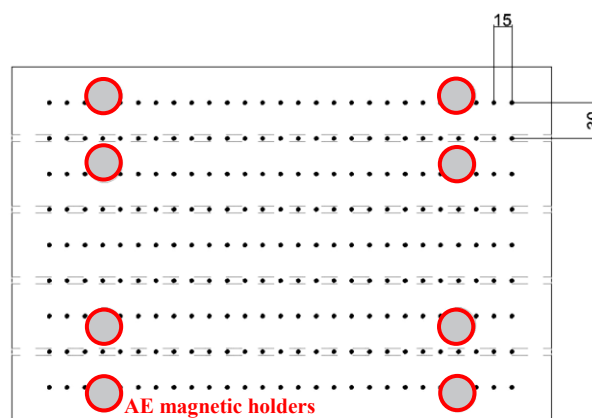


Fig. 3. UPV mapping grid outline, dimensions in mm. The large grey circles stand for the AE sensors' magnetic holders position.

3 Results

3.1 Cracking and networks fracture

The crack onset defines the moment at which the networks are activated since the tubes break under tensile stresses along the bending zone. Based on AE signal strength (feature expressing the wave magnitude) analysis, depicted in Figure 4 for representative samples per series, the early jump in signal strength is attributed to damage mode shift, from strain development and micro-cracking to crack initiation. The black-coloured data points are derived as the average value obtained in an interval of 0.5 kN. This energy rise trend is demonstrated for both the reference series and the series with embedded networks and is indicated in each subfigure with an arrow. Beyond that moment, the cracks widen and propagate along the slab's height, however the signal strength remains at lower levels. Interestingly, the crack onset varies among samples: the energy peak is situated for the reference slab at 13.44 kN (see arrow in Figure 4a); for the conventional network at 9.7 kN (Figure 4b); and for the experimental network configuration at 6.9 kN (Figure 4c). This leads to the conclusion that crack onset appears earlier for the slabs in which networks are embedded, therefore the vascular network introduces a weakening element in the concrete design.

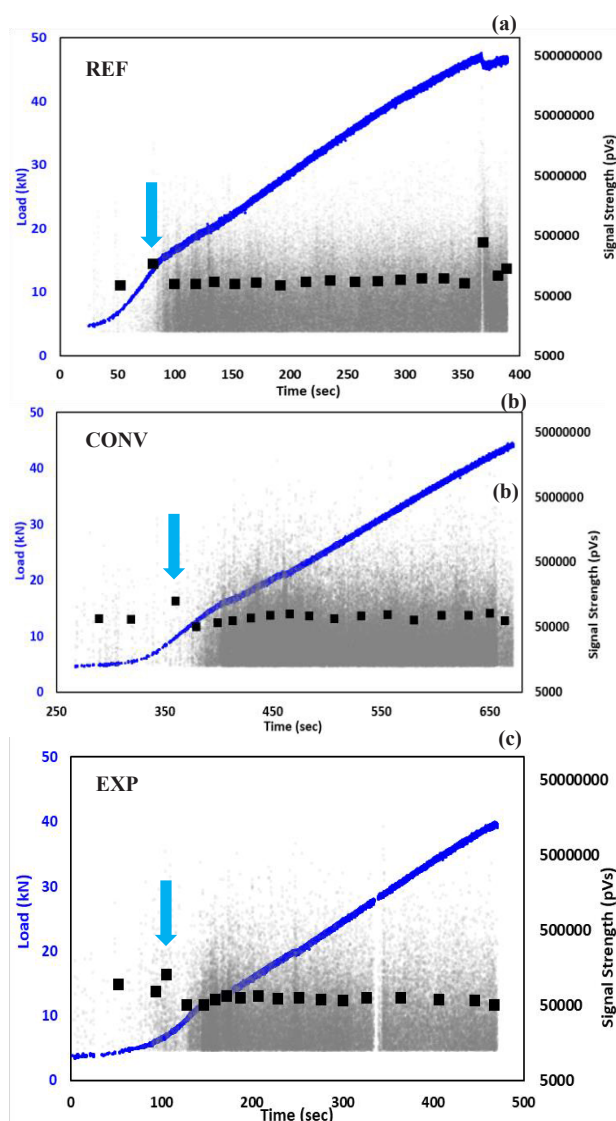


Fig. 4. Signal strength and load plots in time for the: **a)** reference; **b)** conventional; **c)** experimental series. The average values of signal strength at integrals of 0.5 kN are also marked with black-coloured points.

3.2 Cracks filling and AE amplitude recovery

The AE hits collected at the pencil lead breaking calibration test provide an indirect proof of crack filling by stiffened agent and potential healing, as demonstrated in Figure 5 (representative samples per series). The hit's amplitude captured by a sensor after travelling through the cracking zone (data illustrated here for propagation distance of 350 mm) is plotted at discrete moments: in intact state (before cracking) that indicates the intrinsic wave attenuation effect, after cracking, after healing, after the second cracking cycle and after re-healing. For the sake of completeness, the amplitude as captured by the sensor standing next to the pencil lead breaking point (propagation distance 0 mm) is also plotted to provide the amplitude's upper limit. Additionally, the lowest expected amplitude value is set by the threshold of 39 dB.

Comparing the reference series, at which healing is not expected in the series with embedded networks, one may notice significant recovery of the amplitude after healing. It is remarkable that the amplitude is at least 22% and 20% higher in the healed series compared to the reference at the first (both network series) and second healing cycle (experimental series only) respectively.

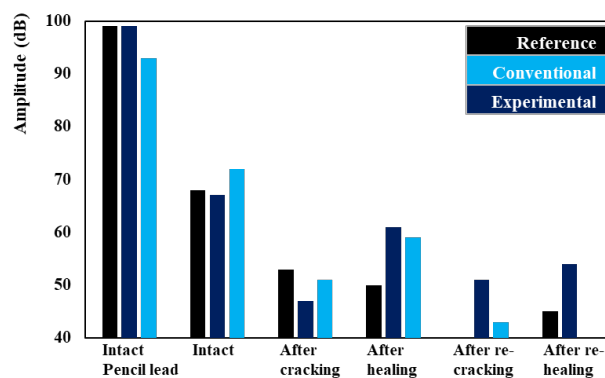


Fig. 5. Signal strength and load plots in time for the: **a)** reference; **b)** conventional; **c)** experimental series (data missing for re-cracking and re-healing stages since a second healing was not attempted).

3.3 The impact of networks on the complex crack patterns

The UPV post-cracking measurements illustrated in planar maps in Figure 6 demonstrate the complexity of cracking for the concrete slabs under investigation. Both reference and healed series develop complex macro-crack patterns with multiple inter-linked branches. The scheme varies when conventional networks are considered: the cracks develop oriented parallel to the networks at the middle bending zone. These unexpected crack branches are linked to the weakening effect that networks introduce at the concrete cover zone. Remarkably, several cracked zones at the middle and

upper zone of the conventional network slab reach a UPV value larger than 3900 m/s (light and dark green), therefore local healing is expected. It should be noted that zones of high velocity are also reported on the reference series, however are limited on intact areas of the slab, therefore stand far away or at the vicinity of the cracks.

Similar to the reference series (Figure 6a), no healing and crack closure is obtained at the edges of the bending zone (Figure 6b), where shear cracks are dominant and develop with larger crack opening. It is concluded that insufficient healing agent was provided at the bending zone edges, therefore the cracks remain widely open after the healing agent treatment.

The UPV recovery is present for the Experimental series (Figure 6c), however less evident since no UPV larger than 3700 m/s is reported at the bending zone. The crack pattern is once again modified with non-symmetric cracks distribution and dominant shear cracks at the right side of the slab. The large shear cracks develop extra inter-linked branches leading to a very dense crack pattern with UPV values often lower than 2500 m/s. It is shown that the experimental networks effectively provide limited healing locally, however their presence enhances the weakening effect on the concrete cover zone.

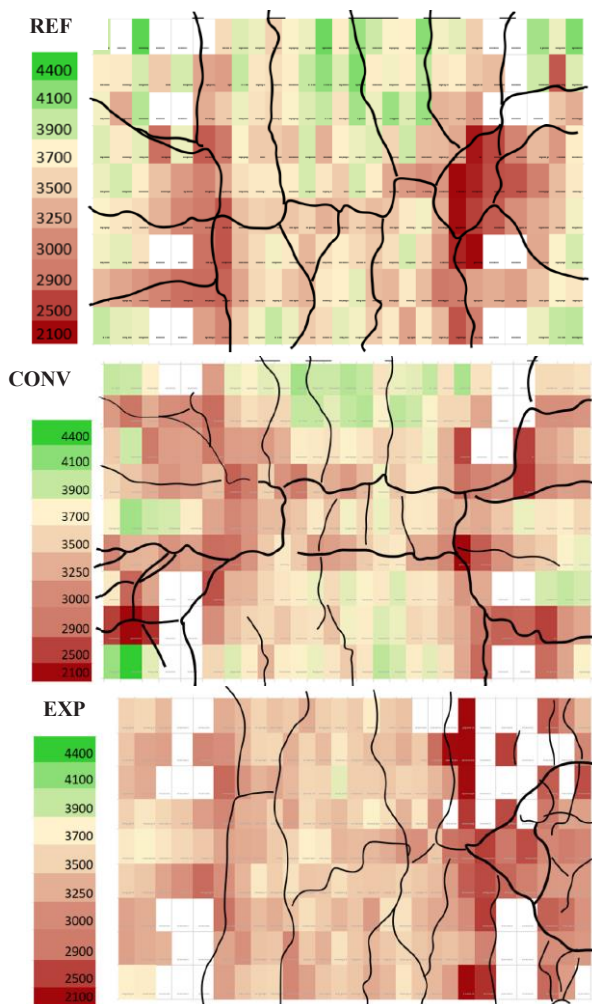


Fig. 6. UPV mapping in a planar projection for the: **a)** reference; **b)** conventional; **c)** experimental series. The crack patterns are also marked in black-coloured lines. Note: the lines thickness should be related to the crack width.

4 Conclusions and Future Work

This preliminary work reports on novel 3D printed vascular networks designed to provide healing in concrete slabs that develop complex crack patterns under bending. A limited recovery of the concrete is demonstrated using advanced elastic wave analyses leading to the conclusion that further design optimization is required. In any case, the inspection methodology effectively localizes the healed zones and pinpoints the mechanical properties restoration after the agent release, providing this way a promising tool for future experimental campaigns.

Financial support of FWO (Fonds Wetenschappelijk Onderzoek-Vlaanderen, 12J7720N (for Tsangouri Eleni)) is gratefully acknowledged. Yasmína Shields acknowledges funding from the European Union's Horizon 2020 research and innovation program under the Marie Skłodowska-Curie grant agreement no. 860006.



References

1. N. De Belie, E. Gruyaert, A. Al-Tabbaa, P. Antonaci, C. Baera, D. Bajare, A. Darquennes, R. Davies, L. Ferrara, T. Jefferson, C. Litina, *Adv. Mater. Inter.* **5**, 17 (2018)
2. Z. Li, L. de Souza, C. Litina, A.E. Markaki, A. Al-Tabbaa, *Mater. Des.* **190** (2020)
3. C. De Nardi, D. Gardner, A. Jefferson, *Materials* **13**, 6 (2020)
4. E. Tsangouri, C. Van Loo, Y. Shields, N. De Belie, K. Van Tittelboom, D.G. Aggelis, *Appl. Sci.* **12**, 10 (2022)
5. Y. Shields, N. De Belie, A. Jefferson, K. Van Tittelboom, *Smart Mater. Struct.* **30**, 6 (2021)
6. L. Ferrara, T. Van Mullem, M.C. Alonso, P. Antonaci, R.P. Borg, E. Cuenca, A. Jefferson, P.L. Ng, A. Peled, M. Roig-Flores, M. Sanchez, *Constr. Build. Mater.* **167** (2018)
7. T. Van Mullem, G. Anglani, M. Dudek, H. Vanoutrive, G. Bumanis, C. Litina, A. Kwiecień, A. Al-Tabbaa, D. Bajare, T. Stryzewska, R. Caspeele, *Sci. Technol. Adv. Mater.* **21**, 1 (2020)
8. P. Minnebo, G. Thierens, G. De Valck, K. Van Tittelboom, N. De Belie, D. Van Hemelrijck, E. Tsangouri, *Materials* **10**, 1 (2017)
9. E. Tsangouri, J. Lelon, P. Minnebo, H. Asaue, T. Shiotani, K. Van Tittelboom, N. De Belie, D.G. Aggelis, D. Van Hemelrijck, *Constr. Build. Mater.* **228** (2019)
10. E. Tsangouri, F.A. Gilabert, N. De Belie, D. Van Hemelrijck, X. Zhu, D.G. Aggelis, *Constr. Build. Mater.* **218** (2019)

11. K. Van Tittelboom, N. De Belie, F. Lehmann, C.U. Grosse, *Constr. Build. Mater.* **28**,1 (2012)
12. A. Bejan, S. Lorente, K.-M. Wang, *J. Appl. Phys.* **100**, 3 (2006)
13. Z. Li, L.R.D. Souza, C.Litina, A.E. Markaki, A. Al-Tabbaa, *Materials* **12**, 23 (2019)
14. E. Vangansbeke, Master thesis at Vrije Universiteit Brussel (VUB)-Architectural Engineering (2023)
15. Y. Shields, T. Van Mullem, N. De Belie, K. Van Tittelboom, *Sustainability*, **13**, 23 (2021)
16. N.N. Hsu, *Mater. Eval.*, **39** (1981)